



Visualization of silica dispersion states in silicone rubber by fluorescent labeling

Kexu Chen¹, Ming Kang^{1,*} , Ai Lu^{1,2}, Lin Chen¹, Lixian Song¹, and Rong Sun¹

¹State Key Laboratory of Environment-Friendly Energy Materials, Southwest University of Science and Technology, Mianyang 621010, Sichuan, China

²Institute of Chemical Materials, China Academy of Engineering Physics, Mianyang 621900, Sichuan, China

Received: 29 September 2018

Accepted: 23 November 2018

Published online:

3 December 2018

© Springer Science+Business Media, LLC, part of Springer Nature 2018

ABSTRACT

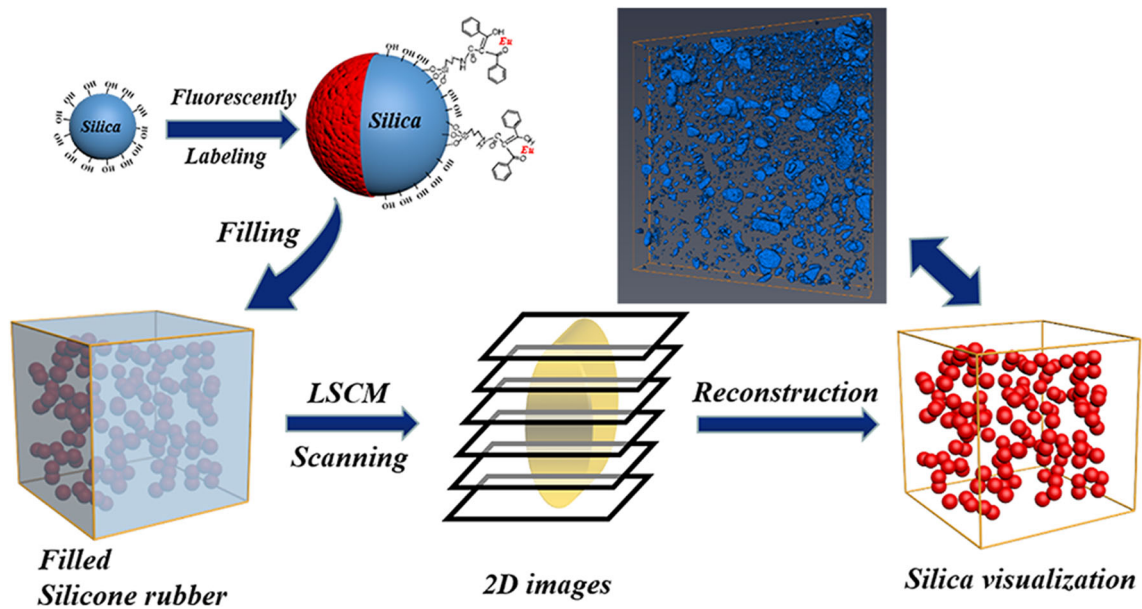
The internal dispersion structure of silica fillers in polymer matrix is significant for design and fabricating high-performance polymer composite. In order to explore the relationship between fillers spatial dispersion states and mechanical properties, we use superficial fluorescent labeling to achieve fillers visualization in polymer matrix with laser scanning confocal microscopy. Through the effect of fluorescent silane coupling agent, the uniform red fluorescence characteristics were shown on the silica surface. The 2D-planar and 3D-spatial dispersion states of silica fillers in rubber matrix can be accurately observed with fluorescence imaging technology. The results by Avizo software statistics show that high-content silica fillers in composite tend to undergo dissociation of aggregates. These dissociated small volume aggregates which facilitate the interaction between particles and rubber matrix to dissipate mechanical energy effectively and rapidly improve rubber toughness. This successful visualization method opens a new avenue in spatial dispersion description of fillers aggregates in organic-inorganic composite.

Introduction

Silica/silicone rubber is an important composite material because of its excellent scalability and high resiliency [1–4]. The silica fillers as a traditional inorganic fillers are widely used in the silicone rubber for improving the mechanical strength and thermal stability [5–7]. However, the premise of achieving these improvements lies in the good dispersion of

silica fillers in the polymer matrix [8–11]. Two common methods to solve the problem are modifying silica fillers or increasing the filler content in polymer [12–14]. Although the support of a series of advanced techniques has been used to evaluate the changes of fillers structure in polymer matrix, such as SEM, AFM, TEM and Nano-CT [15–21], these testing methods are always damaging the sample or taking long test time. The relationship between internal

Address correspondence to E-mail: mkang311@126.com



Scheme 1 Fluorescent labeling of silica and visualization process of silica fillers in polymer composite.

spatial dispersion state and mechanical enhancement is still lacking evaluation criteria [22, 23].

In recent years, combining fluorescence display technology with optical microscopy to visualize internal structure in materials is an effective method [24, 25]. The visualization of convenient and noninvasive is native functionalities for laser scanning confocal microscopy (LSCM) can be widely using in fluorescence detection field. Therefore, the fluorescent properties of materials become the key point to visualization of the dispersion states. The rare earth (RE) materials due to their excellent optical properties have been developed in display technique, optical detection and fluorescent or laser systems [26–28]. However, the conventional prepared method for inorganic optical materials was doped with RE ions in situ, and this also extremely limits the application of inorganic optical materials [29]. Up to now, a kind of special silane coupling agent establishes a bridge to connect RE ions and the surface of inorganic materials [30, 31]. This successful method of fluorescent labeling inorganic materials broadens the application range of optical materials, and proposed a new method to achieve the precise and integrated evaluation for the spatial dispersion state of inorganic fillers in polymer matrix.

In this work, we choose a typical silica/silicone rubber composite to reveal the relationship between the internal dispersion structure of silica fillers and polymer mechanical properties. The silica fillers

(silica G, ~ 200 nm) were first been homogeneous fluorescent labeling with fluorescent silane coupling agent (Eu(DBM-Si)₃) [30]. The as-prepared fluorescent silica fillers (Silica FG) with strong red emission were filled into the silicone rubber matrix. The dispersion of fluorescent silica fillers can be distinctly visualized, and a series of 2D images were acquired by laser scanning confocal microscopy (LSCM). The 3D dispersion state of the fillers was reconstructed with the support of software modeling (Avizo) (Scheme 1). Furthermore, the change of internal dispersion which is different amount of fillers in silicone rubber matrix can be correlated to their mechanical properties. This work also serves to demonstrate that the fluorescent labeling and confocal fluorescence imaging technology are convenient methods to evaluate the internal fillers dispersion, which is also available for large-scale industrial applications and different polymer composite systems.

Experimental

Materials

Dibenzoyl methane (DBM), 3-(triethoxysilyl)-propyl isocyanate (95%, ICP TES), and Eu(NO₃)₃·6H₂O (99.99%) were purchased from Aladdin Reagent Co. Tetraethyl orthosilicate (TEOS) was obtained from Chengdu Kelong Chemical Co, Ltd. Sol-gel

monodisperse silica (referred to as silica G) was prepared on our own using the well-known Stöber method [32, 33]. Silicone rubber (type: 110-2, $M_n = 6.5 \times 10^6$, 0.23% mol⁻¹ vinyl content) was purchased from Zhejiang Xin'an Chemical Group Co., Ltd. (China). Hydroxyl silicone oil (GY-209-3) was used as structure controlling and coupling agent, which was kindly provided by Chenguang Research Institute of Chemical Industry, China. Dicumyl peroxide (DCP, 99%, AR) used as a vulcanization agent was purchased from Chengdu Kelong Chemical Reagent Industry (China). The other materials are all commercially available.

Superficially fluorescently labeling silica fillers

The fluorescent silane coupling agent (Eu(DBM-Si)₃) has been successfully synthesized by our previously reported method [32], which can be fixed on the surface of silica by covalently grafting and achieve fluorescent labeling. The experimental process is as follows: 1 g silica G was activated at 110 °C for 2 h and dispersed in 20 ml solution (anhydrous alcohol: water 3:1, v/v) with ultrasonic dispersion for 30 min. Then, 13% fluorescent silane coupling agent was dissolved in 3 ml anhydrous alcohol and dripped into the silica G dispersion liquid at 50 °C, and the pH of the solution was adjusted to 10 by ammonia. After stirring for 2 h, the solution was centrifuged and washed with anhydrous ethanol and deionized water for several times, respectively. The samples were dried at 60 °C for 24 h in air. The achieved fluorescently labeled silica G was referred to as silica FG.

Fabrication of silica/silicone rubber composite

The silica-filled silicone rubber compound was prepared by two-step mixing method. First, the silicon rubber (30 g), the 10–40 wt% silica FG (3–12 g) and the 8 wt% hydroxyl silicone oil (2.4 g) were mixed together under 105 °C and 90 rpm for 30 min. Subsequently, the mixed silicon rubber was cooled down to room temperature and kept for 1 week to ensure an equilibrium adsorption. Second, the 2.5 wt% cross-linking agent DCP was added into the mixed silicon rubber at room temperature with 90 rpm for 15 min and then was cured to a film by a

compression molding machine at 160 °C and 10 MPa for 10 min to obtain the vulcanizates.

3D dispersion states reconstructed of silica in silicone rubber

To ensure the fluorescent silica-filled silicon rubber and to enable a high-quality analysis of the dispersion, excitation laser was operated to acquire 2D images, and their digital image resolution are up to 1024 × 1024 pixel (Voxel size: $x = 0.568 \mu\text{m}$, $y = 0.568 \mu\text{m}$, $z = 0.148 \mu\text{m}$), during image acquisition from x , y , z three dimensions. All the confocal images were captured in Tiff format, and the test time of nearly 500 consecutive confocal images (image size: $581.25 \times 581.25 \mu\text{m}^2$) was 20 min.

The hundreds images acquitted from LSCM only present fluorescence of silica surface, and so the two phases of silica and rubber do not need to be distinguished. 3D visualization analysis of the acquired images was realized by Avizo Fire VSG software (Visualization Sciences Group, Bordeaux, France). During the reconstructed process, the method and authenticity of imaging are the key factors. The threshold chosen is very important to be close to the real condition [20], which was modified and determined until the calculated volume fraction from 3D images was very close to the theoretical value in filled silicon rubber. Finally, 3D images were obtained through the volume rendering. The 3D images intuitively demonstrate the silica dispersion in silicon rubber, and more information can be calculated by using Label Analysis and Volume Fraction.

Characterization methods

The morphology of silica G and fluorescent silica G was investigated by using field emission scanning electron microscope (FESEM) (TESCAN MAIA3 SEM) equipped with an energy-dispersive spectrometer and transmission electron microscopy (TEM) (Zeiss Libra 200 FE). The photoluminescence excitation and photoluminescence emission spectra of fluorescent silica G were measured by using the luminescence spectrophotometer (Model F-4500, Hitachi) with a 150-W xenon lamp as the excitation source. Mixed rubber was prepared by a laboratory size internal mixer (RC400P, HAAKE Co., Ltd, Germany). Cross-linked silicone rubber sheets were prepared in a platen press (P300E, DR COLLIN Co.,

Ltd, Germany). 2D image acquisition and 3D reconstruction were produced using confocal laser scanning microscopy (Leica TCS Sp8) and Avizo Fire VSG software, respectively. The tensile tests were performed at room temperature on RSA-G2 (TA Instruments) according to ISO 37 S3A.

Results and discussion

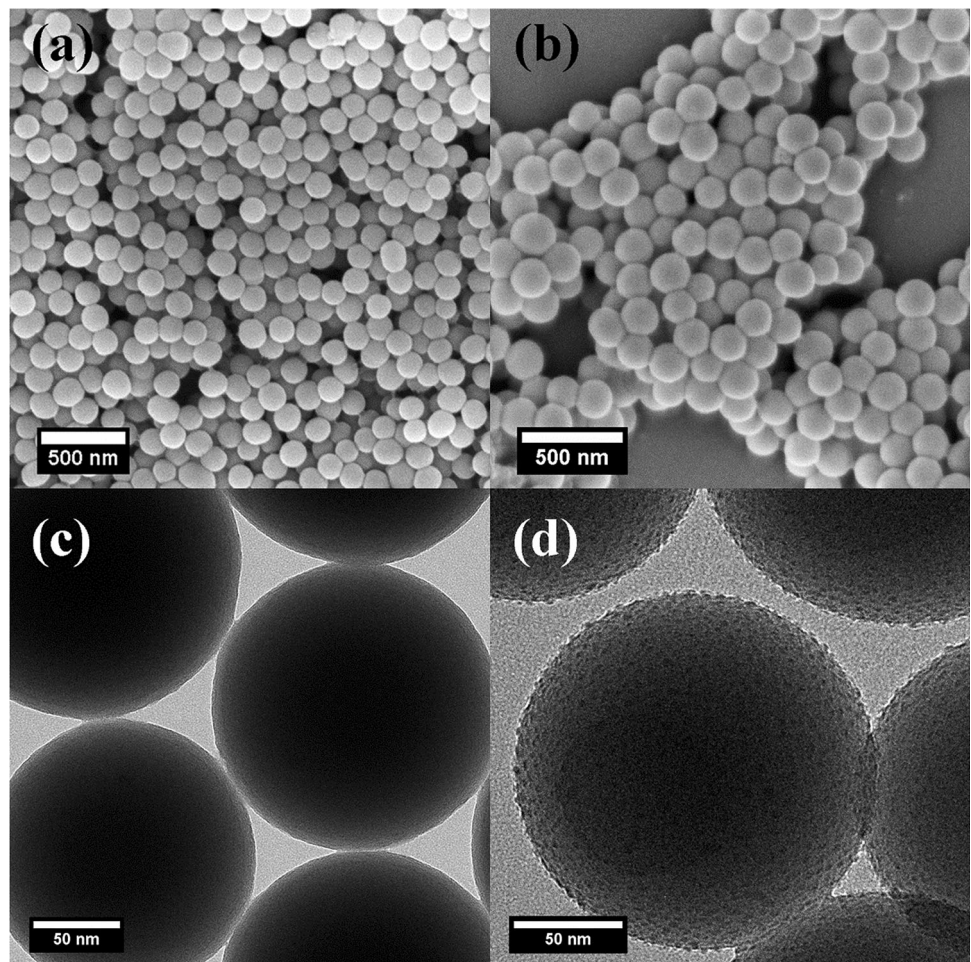
Characterization and fluorescence properties of fluorescent silica

The morphology and particles size dispersion of pure silica (silica G) and fluorescent silica (silica FG) were investigated by SEM. As shown in Fig. 1a, the silica G synthesized through the well-known Stöber method was well dispersed and uniform with a diameter of ~ 200 nm, and its surface structure is very smooth. Similarly, the silica FG was still spherical and monodispersed, but its surface does not seem very

smooth as shown in Fig. 1b. To further understand the detailed information of silica G surface structure, TEM observations were also performed as shown in Fig. 1c, d. Obviously, compared with silica G, the surface of silica FG replaces smooth one. These results can be considered that alkoxy silane group of fluorescent silane coupling agent uniformly bonds with each silica G surface successfully.

From the ^1H NMR of silane coupling agent which was modified on silica surface, the characteristic chemical shifts can be clearly identified (Fig. 2a). In addition, the element composition of silica FG through X-ray photoelectron spectroscopy (XPS) and the results are shown in Fig. 2b. The results of survey spectrum confirm the presence of carbon (C), silicon (Si), oxygen (O), nitrogen (N) and europium (Eu) elements, and the peak areas also reflect the elemental content. To further explain the elemental distribution states of fluorescent labeling on silica FG,

Figure 1 SEM and TEM of silica G (a, c) and silica FG (b, d).



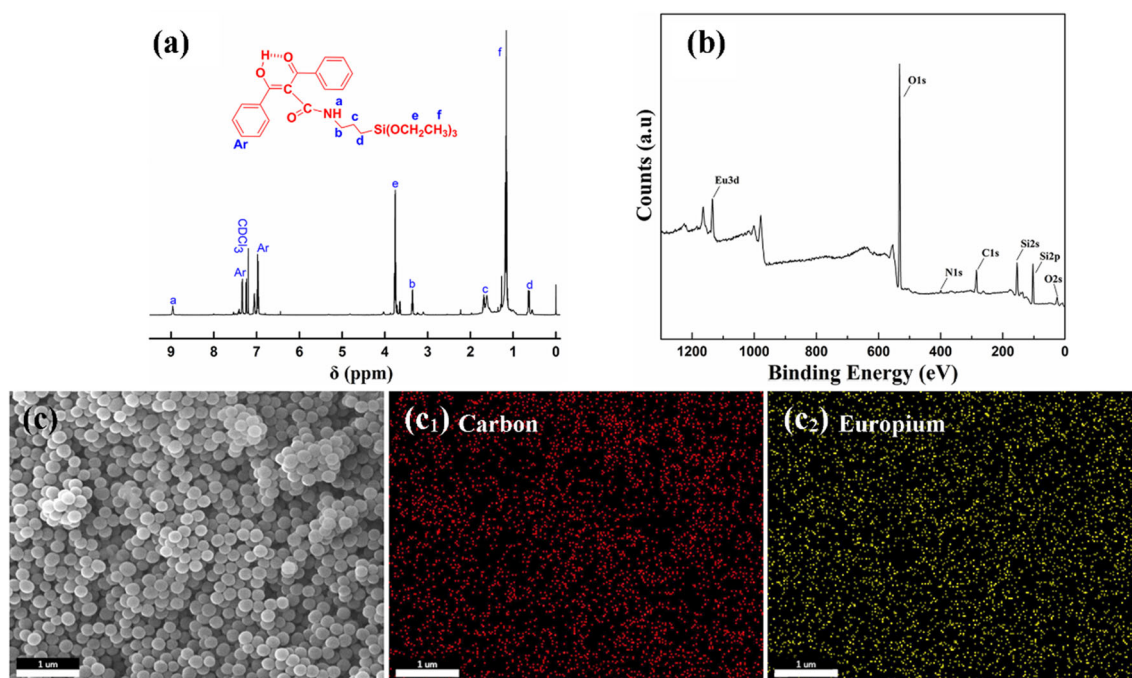


Figure 2 ^1H NMR spectrum of functional silane coupling agent which fixed on silica surface (a), XPS survey spectrum of silica FG (b), EDX element mapping of silica FG (carbon (C₁) and europium (C₂) indicate the range of element distribution).

the EDX elemental mapping was also employed to describe the surface elements distribution of silica FG (Fig. 2). The carbon and europium as representative elements were marked red and yellow point to indicate the range of element distribution. The results are highly consistent with the elements of the fluorescent silane coupling agent on silica FG surface, and strongly prove that the surface of silica can be uniformly fluorescently labeled through this fluorescent labeling method.

In order to guarantee the highly efficient fluorescence of the silica FG, the amount of fluorescent silane coupling agent for modification was optimized in the range of 5–17%. Limited by surface area, the fluorescence intensity of silica G has an optimal value at 13%. The detailed fluorescence spectra are shown in Fig. 3. These data suggest that the silica G surface is a homogeneous fluorescent functionalization, and it laid the foundation for the evaluation of spatial dispersion state in polymer matrixes.

2D and 3D images acquisition of fluorescent silica

Under the excitation of UV energy, the basic principle used to reveal the superficial energy conversion of silica FG and the 2D images acquisition method is

illustrated in Fig. 4. The absorption wavelength (λ_{abs}) converted to the emission wavelength (λ_{em}) is attributed to fluorescent silane coupling agent of silica FG surface. Because of the interaction of hydrogen bonds among the abundant silanol groups on silica surface, the silica combine into aggregates in rubber matrix [34]. However, the silica particles inside the aggregates are only in contact with each other, and the change in the environment of the rare earth ions on silica surface is not obvious. Therefore, the subtle changes in their concentration are not enough to cause dissipation of excitation energy at the emission level by cross-relaxation between rare earth ions and reduced fluorescence performance [35]. These surface luminescence information of silica aggregates can be obtained by LSCM scanning.

The effectiveness of fluorescent labeling is quite important to ensure that silica aggregates can be observed by LSCM and represent the dispersion state in the rubber matrix. As obtained from LSCM images, the fluorescent image and overlapping can be observed, representing the silica FG. The bright red emission of silica FG can be observed under the excitation of 405-nm laser irradiation (Fig. 5a). Meanwhile, the red and dark areas are attributed to silica FG and rubber phases, respectively. The overlapping image demonstrates the observed

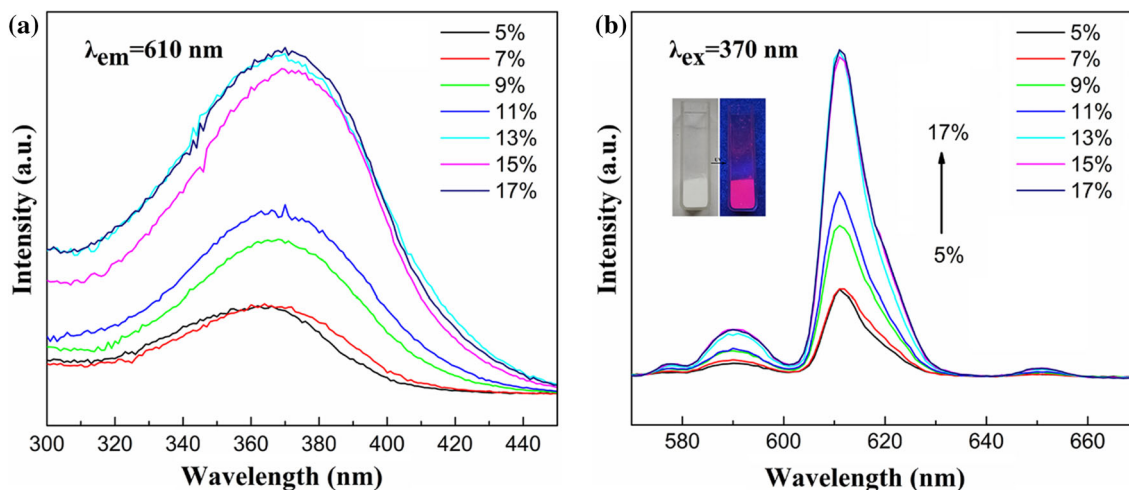


Figure 3 Excitation (a) and emission (b) spectra of silica FG with fluorescent silane coupling agent content in range of 5–17%, the insets show the photograph of silica FG under 365 nm UV light.

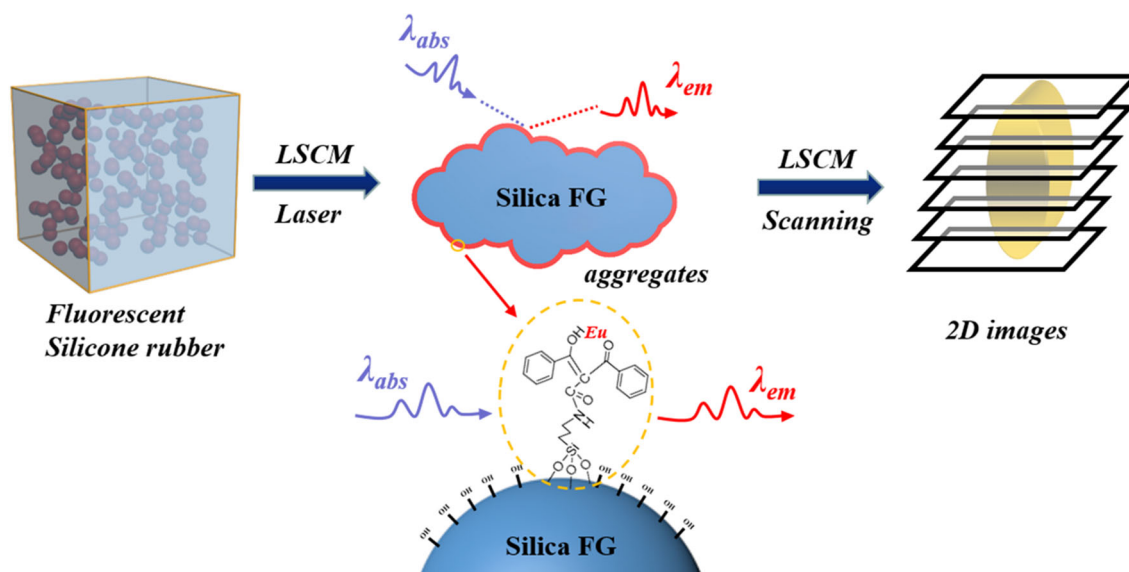


Figure 4 Schematic drawing illustrating the use of fluorescent silane coupling agent to label silica G. Energy can be converted to visible light that only occurs on the surface of silica G and the 2D image acquisition by LSCM scanning through the x , y , and z axes.

luminescence originates from silica FG in rubber matrix (Fig. 5c).

The obvious fluorescence performance of silica FG in rubber matrix implies the great potential to evaluate the dispersion state of silica in the polymer matrix. In our work, more than 400 pieces of the 2D consecutive confocal images are accurately obtained at different focal planes in the silica FG/rubber composite through the optical sectioning (Fig. S1). The 3D images can be reconstructed through Avizo Fire VSG software (Visualization Sciences Group, Bordeaux, France) based on a series of 2D consecutive

confocal images to reflect the 3D architectures and spatial dispersion state in the composite. The 3D median filtering and interactive thresholding was selected to reduce the noise and adjust the imaging threshold of images. This condition was used to get close to the real situation, and determine the same threshold to construct 3D images of silica FG. Figure 6 shows the 3D images of the silica FG/silicone rubber composite with silica FG 10–40 wt%, respectively. The images provide a direct visual observation of the silica in the rubber matrix, and the number of the emission aggregates increased which can be

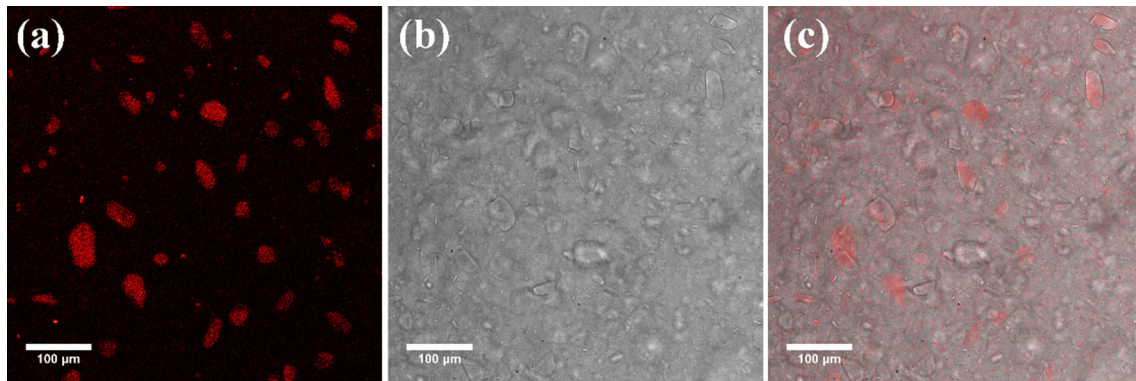


Fig. 5 Confocal fluorescence microscopy images of silica/silicon rubber with 40 wt%: **a** fluorescent image, **b** bright-field optical image, **c** overlapping.

observed with the increased content of silica FG (Fig. 6a–d). These obvious aggregates are due to the interaction of abundant silanol groups on silica surface. Therefore, the silica with different aggregate sizes can be easily distinguished and the spatial dispersion is legibly visualized (Fig. 6a₁–d₁). In addition, the cross-sectional images of rubber composite also show a similar distribution state (Fig. S2) and the result indicated that the 3D fluorescence visualization could show the real dispersion state in the composites.

Moreover, the aggregates volume of different silica contents in rubber matrix can be counted directly by Avizo software. For all samples, the volumes of aggregates are mainly less than $200 \mu\text{m}^3$, and the

large volume gradually shifts to small volume from 10 to 40 wt% (Fig. 7a–d). Thus, the change in silica aggregates has caused our widespread concern. The aggregate volumes smaller than $10 \mu\text{m}^3$ and larger than $200 \mu\text{m}^3$ (denoted as *Ps* and *PL*) were selected to evaluate the aggregation degree of aggregates (Fig. 7e). The different contents of silica fillers in silicon rubber affect *Ps* and *PL*. For 10 wt% silica fillers in silicon rubber, *Ps* is about only 23.6%, which reaches 84.5% in 40 wt%. Meanwhile, *PL* decreases from 37.4% in 10 wt% to 4.7% in 40 wt%. The synchronous changing trends of *Ps* and *PL* reveal that the high-content silica tend to undergo aggregates release, which is conducive to the formation of small volume aggregates.

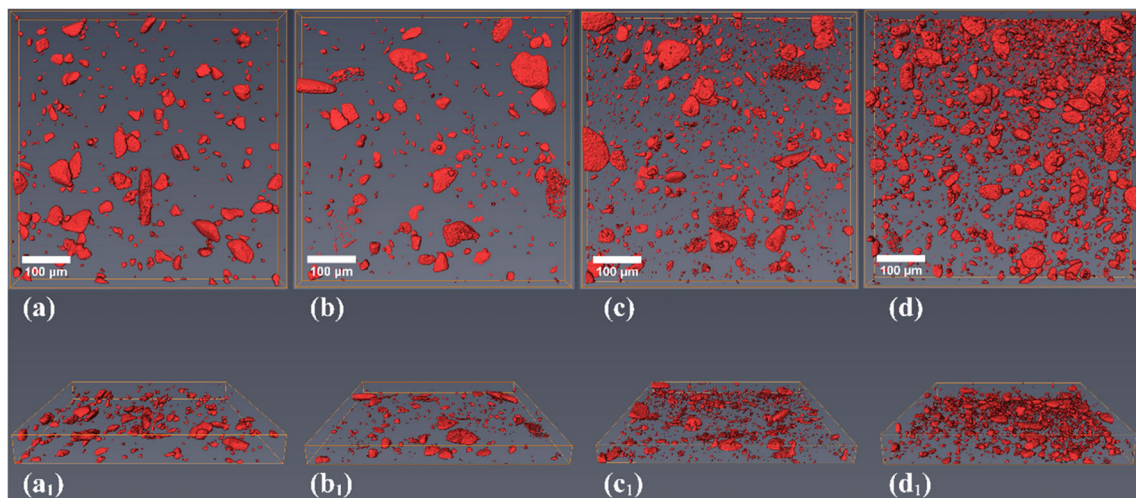


Fig. 6 The 3D reconstruction images of the silica FG dispersed in rubber composite with different contents: (a, a₁) 10 wt%; (b, b₁) 20 wt%; (c, c₁) 30 wt%; (d, d₁) 40 wt%.

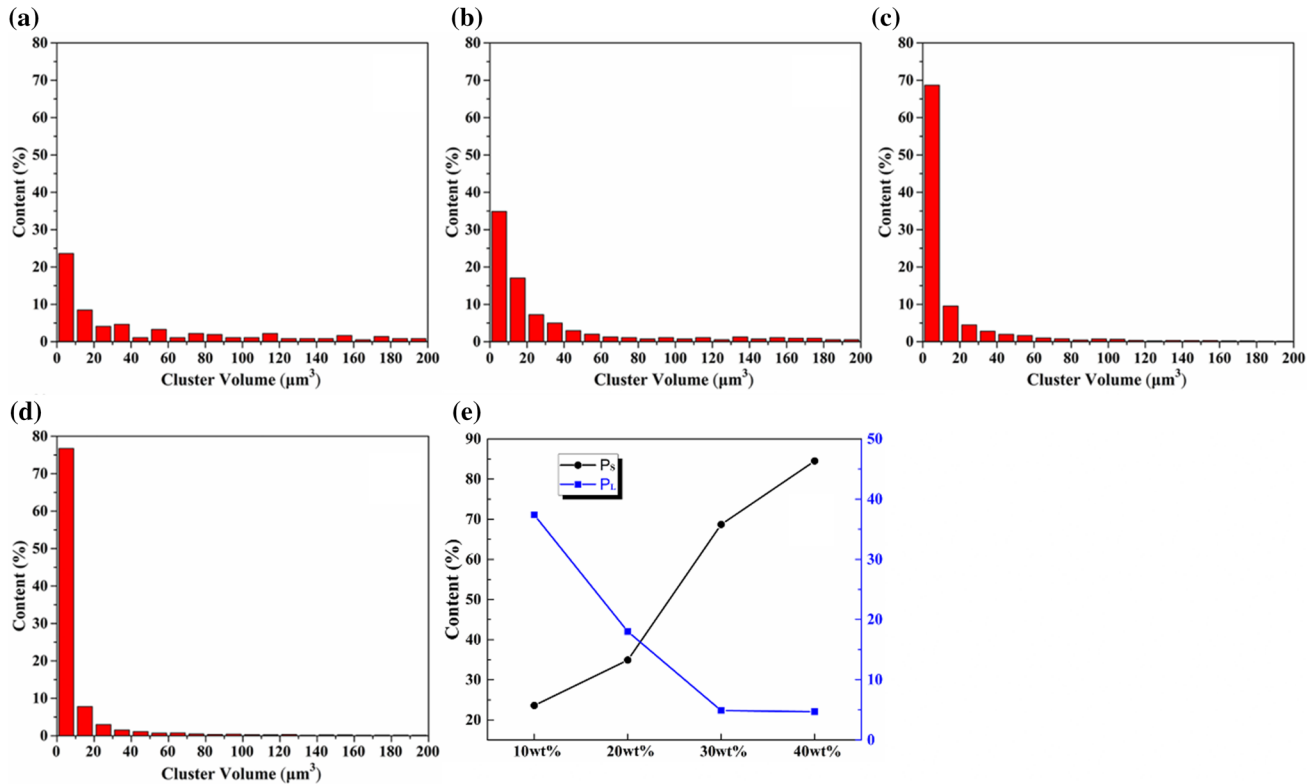


Fig. 7 a–d The size distribution of silica aggregates obtained from with silica FG contents 10–40 wt%; e contents of aggregates with sizes smaller than 10 μm^3 (P_s) and larger than 200 μm^3 (P_L).

Tensile and mechanical fracture measurements

The mechanical properties of fluorescent labeled silica (silica FG) and silica G have no obvious difference through the typical content loading (40 wt%) to fill into silicon rubber matrix (Fig. S3). Therefore, the fluorescently labeled silica can effectively reflect the dispersion state of the actual silica in the silica/silicon rubber composite.

On the base of this condition, the mechanical properties of silica/silicon rubber composite with different silica FG content loadings (0–40 wt%) were compared. For a quantitative comparison, besides the stress–strain curves during tensile deformation (Fig. 8a), we calculated the fracture energy Γ of all samples, which is the work required to generate a crack on unit area of sample and expressed as [21, 36]:

$$\Gamma = L_0 \int_0^{\varepsilon} \sigma(\varepsilon) d(\varepsilon)$$

where $\sigma(\varepsilon)$ is the tensile stress at strain of ε and L_0 is the initial section width of sample (2 mm).

The fracture energy Γ of composite was calculated from 41.78 (0 wt%) to 246.96 J m^{-2} (40 wt%) as shown in Fig. 8b, and the fracture energy of 40 wt% increases by 591%. The obvious toughening effect is attributed to the dispersion of silica particles in rubber and the interaction among each other. Although the composite generates continuous reinforcement and toughening effects with the increase in silica content in rubber matrix, the fracture energy increment of 10–20 wt% (55.6 J m^{-2} and 82.08 J m^{-2}) is less than 30–40 wt% (139.12 J m^{-2} and 246.96 J m^{-2}). According to the internal structure, the increase in small volume silica improves the interaction among the particles, and larger specific surface area can better combine with rubber matrix. The interaction between silica particles and rubber or particles can effectively dissipate mechanical energy, which may account for rapid improvement in toughness.

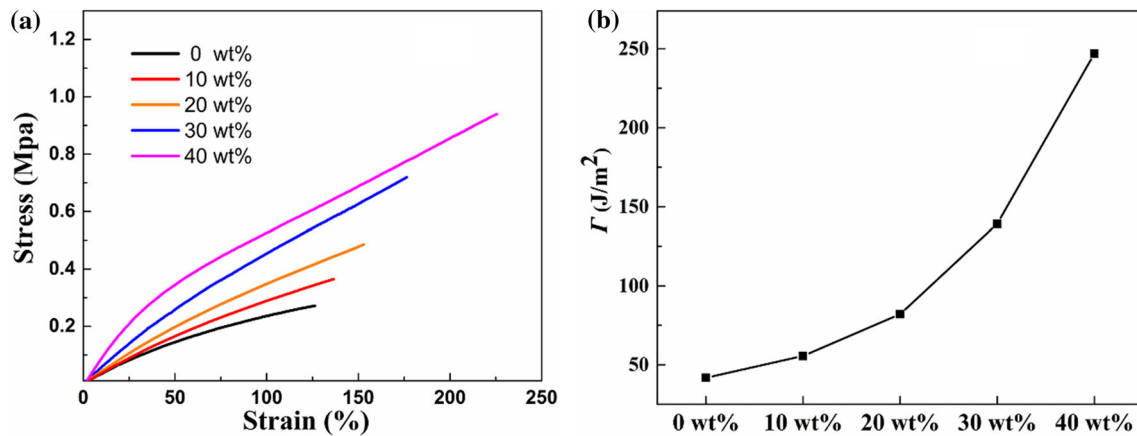


Fig. 8 **a** Engineering stress–strain curves obtained with silica FG contents 0–40 wt% and **b** calculated value of fracture energy.

Conclusions

We have successfully achieved the homogeneous fluorescent labeling of silica using fluorescent silane coupling agent (Eu(DBM-Si)₃). The obtained fluorescent silica exhibits a strong red emission with the optimized labeling content in 13% for Eu(DBM-Si)₃. Through the LSCM imaging method, the 3D spatial dispersion of silica fillers in the silicon rubber matrix was reconstructed which guaranteed effective application as a fluorescent labeling to reveal the dispersion state in the polymer matrix. The silica aggregates in the rubber matrix of which volumes are smaller than 10 μm³ from 23.6 to 84.5% with the content of silica fillers increased in the composite. At the same time, the fracture energy increased from 55.6 to 246.96 J m⁻². Significant improvement in mechanical properties is attributed to small-sized silica particles which facilitate the interaction among particles or the silicone rubber matrix, and the rubber toughness is reinforced through effectively dissipating mechanical energy. This proposed strategy in our study was implemented based on the industrial standardized processing methods which provided the great possibilities to establish the relationship between fillers spatial dispersion structure and performance of polymers matrix.

Acknowledgements

This work was supported by the Sichuan Science and Technology Support Project in China (2017GZ0126).

Electronic supplementary material: The online version of this article (<https://doi.org/10.1007/s10853-018-03191-z>) contains supplementary material, which is available to authorized users.

References

- Valentín JL, Morabarrantes I, Carreterogonzález J, Lópezmanchado MA, Sotta P, Long DR, Saalwächter K (2010) Novel experimental approach to evaluate filler-elastomer interactions. *Macromolecules* 43:334–346
- Bouty A, Petitjean L, Degrandcourt C, Gummel J, Kwaśniewski P, Meneau F, Boué F, Couty M, Jestin J (2014) Nanofiller structure and reinforcement in model silica/rubber composites: a quantitative correlation driven by interfacial agents. *Macromolecules* 47:5365–5378
- Davris T, Mermetguyennet MRB, Bonn D, Lyulin AV (2016) Filler size effects on reinforcement in elastomer-based nanocomposites: experimental and simulational insights into physical mechanisms. *Macromolecules* 49:7077–7087
- Klüppel M (2003) The role of disorder in filler reinforcement of elastomers on various length scales. *Adv Polym Sci* 164:1–86
- Landry CJ, Coltrain BK, Wesson JA, Zumbulyadis N, Lippert JL (1992) Polymerization of tetraethoxysilane in polymers: chemical nature of the interactions. *Polymer* 33:1496–1506
- Yang F, Ou Y, Yu Z (2015) Polyamide 6/silica nanocomposites prepared by in situ polymerization. *J Appl Polym Sci* 69:355–361
- Suzuki N, Zakaria MB, Chiang YD, Wu KCW, Yamauchi Y (2012) Thermally stable polymer composites with improved transparency by using colloidal mesoporous silica

- nanoparticles as inorganic fillers. *Phys Chem Chem Phys* 14:7427–7432
- [8] Rittigstein P, Priestley RD, Broadbelt LJ, Torkelson JM (2007) Model polymer nanocomposites provide an understanding of confinement effects in real nanocomposites. *Nat Mater* 6:278–282
- [9] Chandran S, Begam N, Padmanabhan V, Basu JK (2014) Confinement enhances dispersion in nanoparticle-polymer blend films. *Nat Commun* 5:3697
- [10] Mangal R, Srivastava S, Archer LA (2015) Phase stability and dynamics of entangled polymer-nanoparticle composites. *Nat Commun* 6:7198
- [11] Suter JL, Groen D, Coveney PV (2015) Chemically specific multiscale modeling of clay-polymer nanocomposites reveals intercalation dynamics. *Tactoid Self-Assembl Emerg Mater Prop Adv Mater* 27:966–984
- [12] Zhang C, Tang Z, Guo B, Zhang L (2018) Significantly improved rubber-silica interface via subtly controlling surface chemistry of silica. *Compos Sci Technol* 156:70–77
- [13] Zhong B, Jia Z, Hu D, Luo Y, Jia D (2015) Reinforcement and reinforcing mechanism of styrene-butadiene rubber by antioxidant-modified silica. *Compos Part A-Appl S* 78:303–310
- [14] Liu D, Song L, Song H, Chen J, Tian Q, Chen L, Sun G (2018) Correlation between mechanical properties and microscopic structures of an optimized silica fraction in silicone rubber. *Compos Sci Technol* 165:373–379
- [15] Chen L, Song L, Li J, Chen P, Huang N, Li L (2016) From the volume - filling effect to the stress-bearing network: the reinforcement mechanisms of carbon black filler in natural rubber. *Macromol Mater Eng* 301:1390–1401
- [16] Choi S (2010) Improvement of properties of silica-filled natural rubber compounds using polychloroprene. *J Appl Polym Sci* 83:2609–2616
- [17] Baeza GP, Genix AC, Degrandcourt C, Gummel J, Mujtaba A, Saalwächter K, Oberdisse J (2014) Studying twin samples provides evidence for a unique structure-determining parameter in simplified industrial nanocomposites. *ACS Macro Lett* 3:448–452
- [18] Tohsan A, Kishi R, Ikeda Y (2015) A model filler network in nanocomposites prepared by in situ silica filling and peroxide cross-linking in natural rubber latex. *Colloid Polym Sci* 293:2083–2093
- [19] Chen L, Zhou W, Lu J, Li J, Zhang W, Huang N, Li L (2015) Unveiling reinforcement and toughening mechanism of filler network in natural rubber with synchrotron radiation x-ray nano-computed tomography. *Macromolecules* 48:7923–7928
- [20] Zhou W, Chen L, Lu J, Qi Z, Huang N, Li L, Huang W (2014) Imaging the strain induced carbon black filler network structure breakage with nano X-ray tomography. *RSC Adv* 4:54500–54505
- [21] Song L, Wang Z, Tang X, Chen L, Chen P, Yuan Q, Li L (2017) Visualizing the toughening mechanism of nanofiller with 3D X-ray nano-ct: stress-induced phase separation of silica nanofiller and silicone polymer double networks. *Macromolecules* 50:7249–7257
- [22] Brüning K, Schneider K, Roth SV, Heinrich G (2012) Kinetics of strain-induced crystallization in natural rubber studied by WAXD: dynamic and impact tensile experiments. *Macromolecules* 45:7914–7919
- [23] Bindu P, Thomas S (2013) Viscoelastic behavior and reinforcement mechanism in rubber nanocomposites in the vicinity of spherical nanoparticles. *J Phys Chem B* 117:12632–12648
- [24] Guan W, Wang S, Lu C, Tang BZ (2016) Fluorescence microscopy as an alternative to electron microscopy for microscale dispersion evaluation of organic-inorganic composites. *Nat Commun* 7:11811
- [25] Feng Z, Zhong J, Guan W, Tian R, Lu C, Ding C (2018) Three-dimensional direct visualization of silica dispersion in polymer-based composites. *Analyst* 143:2090
- [26] Yuan B, Song Y, Sheng Y, Zheng K, Huo Q, Xu X, Zou H (2014) Luminescence properties and energy transfer of $\text{Ca}_2\text{Mg}_{0.5}\text{AlSi}_{1.5}\text{O}_7$: Ce^{3+} , Eu^{2+} phosphors for UV-excited white LEDs. *Powder Technol* 253:803–808
- [27] Comby S, Surender EM, Kotova O, Truman LK, Molloy JK, Gunnlaugsson T (2014) Lanthanide-functionalized nanoparticles as MRI and luminescent probes for sensing and/or imaging applications. *Inorg Chem* 53:1867–1879
- [28] Li Q, Lin J, Wu J, Lan Z, Wang Y, Peng F, Huang M (2013) Improving photovoltaic performance of dye-sensitized solar cell by downshift luminescence and p-doping effect of Gd_2O_3 : Sm^{3+} . *J Lumin* 134:59–62
- [29] Qiao Y, Chen H, Lin Y, Yang Z, Cheng X, Huang J (2011) Photoluminescent lanthanide-doped silica nanotubes: sol-gel transcription from functional template. *J Phys Chem C* 115:7323–7330
- [30] Chen K, Kang M, Liu M, Shen S, Sun R (2018) Synthesis of di-functional ligand and fluorescently labeling SiO_2 microspheres. *Opt Mater* 79:464–469
- [31] Li WX, Zheng YS, Cao XF, Bai J, Fu ZF, Bao JR, Li YL (2016) Preparation, characterization, and luminescence properties of dysprosium perchlorate with MABA-Si and phen or dipy complexes as well as $\text{SiO}_2@Dy$ (MABA-Si)L core-shell structure nanometer luminescent composites. *J Lumin* 178:470–478
- [32] Mou Y, Kang M, Wang F, Liu M, Chen K, Sun R (2017) Synthesis and luminescent properties of monodisperse $\text{SiO}_2@SiO_2:Eu(\text{DBM})_3$ phen microspheres with core-shell

- structure by sol–gel method. *J Sol–Gel Sci Technol* 83:447–456
- [33] Stöber W (1968) A. Fink and E. Bohn, Controlled growth of monodisperse silica spheres in the micron size range. *J Colloid Interface Sci* 26:62–69
- [34] Wang J, Jia H, Ding L, Xiong X (2015) Impacts of filler covalent and non-covalent modification on the network structure and mechanical properties of carbon-silica dual phase filler/natural rubber. *Polym Adv Technol* 26:1168–1175
- [35] Moretti E, Bellotto L, Basile M, Malba C, Enrichi F, Benedetti A, Polizzi S (2013) Investigation on the effect of Tb (dbm)₃phen on the luminescent properties of Eu (dbm)₃phen-containing mesoporous silica nanoparticles. *Mater Chem Phys* 142:445–452
- [36] Sun JY, Zhao X, Illeperuma WR, Chaudhuri O, Oh KH, Mooney DJ, Vlassak JJ, Suo ZG (2012) Highly stretchable and tough hydrogels. *Nat* 489:133–136